Laser-matter coupling mechanisms governing particulate-induced damage on optical surfaces

M. J. Matthews[1], E. Feigenbaum[1], S.G. Demos[2], R. N. Raman[1], S. R. Qiu[1], N. Shen[1], C. Harris[3], R. A. Negres[1], M. Norton[1], D. Cross[1] and A. M. Rubenchik[1]

[1]*Lawrence Livermore National Laboratory, Livermore, CA 94550, USA*
[2]*Laboratory for Laser Energetics, University of Rochester, Rochester NY 14623*
[3]*Department of Physics, Florida A&M University, Tallahassee FL 32307*

ABSTRACT

A comprehensive study of laser-induced damage associated with particulate damage on optical surfaces is presented. Contaminant-driven damage on silica windows and multilayer dielectrics is observed to range from shallow pitting to more classical fracture-type damage, depending on particle-substrate material combination, as well as laser pulse characteristics. Ejection dynamics is studied in terms of plasma emission spectroscopy and pump-probe shadowgraphy. Our data is used to assess the momentum coupling between incident energy and the ejected plasma, which dominates the laser-particle-substrate interaction. Beam propagation analysis is also presented to characterize the impact of contaminant-driven surface pitting on optical performance.

Keywords: Contamination, damage, plasma generation, particle ejection, energy coupling mechanism, pulsed lasers, surfaces, light scattering

INTRODUCTION

The impact of contaminant particles in an optical system can range from moderate system degradation via optical scattering loss, to catastrophic, as couplers of laser energy into the optic surface sufficient to cause damage [1-11]. A comprehensive study is needed to clarify the energy coupling mechanisms involved and lead the way towards effective mitigation techniques [12, 13]. We propose here a study of the morphological and chemical evolution of surface-bound, micron-scale particles in the presence of high power laser irradiation and their interaction with an underlying optical surface. Fused silica, sapphire and multilayer dielectric (MLD) coatings are the primary optical materials used to host the surface-bound particulates. The approach taken in this study is based on developing a suite of experimental and computational tools that can be used to examine particle-driven damage events in situ and under a wide variety of conditions. The probability of damage for both fused silica optics and dielectric mirrors contaminated with metal and glass particulates was measured and analyzed. Theoretical analysis is used to rationalize the results of laser-particle-induced damage. Electromagnetic wave propagation analysis was simulated using finite difference time domain methods (FDTD), and also estimated using paraxial approximations. Highlights of the accomplishments of this comprehensive study are presented below.

1. EXPERIMENTAL DETAILS

Polished UV-grade Corning 7980 fused silica and multilayer SiO_2/HfO_2 thin film samples were used in the present study, 10 mm thick by 51 mm diameter round. Samples were sol gel anti-reflectance coated (71 nm thickness) for 351 nm transmission. With the exception of silica, Ti and pure Al, particles of various sizes were created by using a cleaned, hardened steel file on the

materials of interest. These filed particles were captured directly into a stack of two precision sieves. The sieve ranges were 38 μm and 55 μm. The silica particles were generated using 351 nm laser ablation and captured directly onto a silica test window. The remaining particle materials were deposited onto separate fused silica substrate samples from a height of approximately 30 cm. The substrates were then taken, rotated 90 degrees such that the substrate surface was parallel to the gravity vector, and mechanically tapped to remove the larger and looser particles resulting in a final surface density of ~1 particle/mm^2. Samples were loaded individually into a large aperture 351 or 1053 nm laser damage test chamber [1] or a small aperture 355 nm test setup [6]. Briefly, a 27 mm diameter, flat-top laser beam with 15-20% beam contrast (ratio of standard deviation to mean) was used with the particles arranged on the incident surface of the sample. Following a ~1 mTorr pump down, all experiments were performed in 2.5 torr of Ar gas. Pulses were shaped using a programmable front end seed pulse system resulting in a 10ns, 0.2 GW/cm^2 pre-pulse immediately followed by a 2.5ns, 2.2 GW/cm^2 shock pulse. This shape was chosen to roughly approximate an ICF pulse shape used on NIF [14]. Local irradiance could be determined using a near field camera registered to a CW illuminated transmission camera. In addition, one cycle of loading and unloading the sample into the laser test chamber was performed, without firing the laser, to help ensure that particles that may have been ejected by laser shots were not mistaken for those that fell off unintentionally during sample handling.
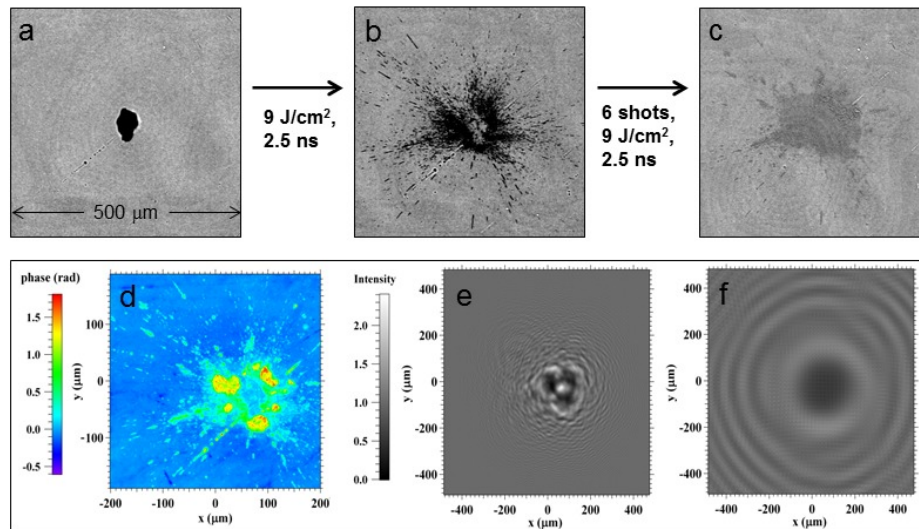

Figure 1: Location of a Delrin™ microparticle on the input surface of a fused silica optic prior to laser shot (a) following a 351 nm, 2.5 ns long, 9 J/cm² laser pulse (b) and following 6 laser shots at 351 nm, 2.5 ns long, 9 J/cm². Following laser shot experiments, the surface height of the sample at the same location was measured using a white light interferometer resulting and used to simulate a phase map (d) which was then input into a paraxial propagation code to simulate 351 nm light intensification at 10 mm € and 100 mm (f) propagation distances.

2. RESULTS AND DISCUSSION

Due to the generally greater impact of plasma generation on the exit surface, damage initiation into a fused silica optic surface tends to be more likely on the exit surface [15]. For this reason, more attention has been given to exit surface contaminant-driven damage initiation but with little attention given to particle-surface energy coupling. In particular, the degree of melting/pitting following a laser cleaning event compared with the more classic fracture-type damage has not been fully assessed. While the contaminant may have been removed, the shallow features in the surface that remain can lead to various levels of propagated intensity modulation due to incident phase modulation which, in turn, may lead to damage [10, 11].

An example of this effect is shown in Figs. 1 (a-c) where polymer particle contamination leads to shallow ablation pits under pulsed laser irradiation. The image in Fig. 1(c) shows a faint pitted region after 6 laser pulses, although the morphology was essentially constant for these particles through laser pulses 4-6. While only acetal homopolymer (Delrin[TM]) is shown, metallic particles behaved similarly in terms of pitting depths and material dispersal, while the PET-G and glass particles pitted less and dispersed more readily.

Figures 1(d-f) shows the simulated phase at z=0 (d) and predicted field intensity in the near field at 10 mm (e) for the laser-induced phase object corresponding to Fig. 1(c). Bearing in mind that the phase map is inversely related to the surface height, Fig. 1(d) clearly reflects the initial material spreading behavior shown in Fig. 1(b) (and observed for aluminum and steel) which tended to leave a locally raised center (depressed phase) relative to the pitted areas. As compared to the z=10 mm intensity pattern consistent with Fresnel diffraction which shows a ~2× intensification which could cause damage exit surface damage on a 10mm thick optic, the z=100 mm [Fig. 1(f)] Fraunhofer diffraction in the far field is only ~1.1× and less likely to cause damage. This correlation of particle size, material type and laser parameters with subsequent beam modulation can be useful in guiding systems designs to allow optics to stay outside likely intensification positions.
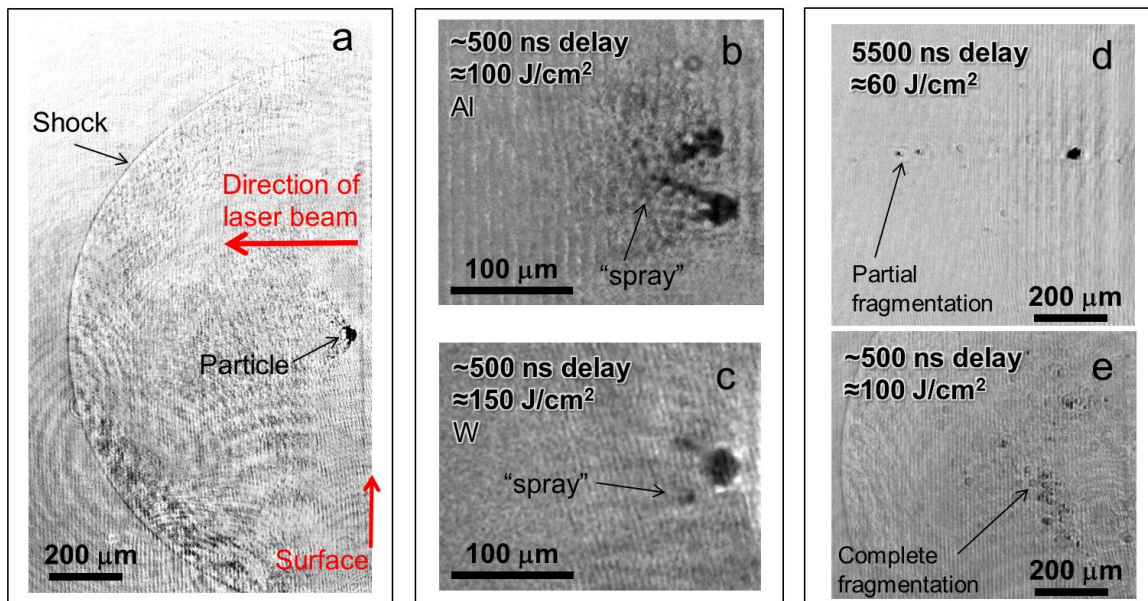

Figure 2: Time-resolved SV images capture the main features observed following the irradiation by a laser pulse of ~30 μm diameter metal particles. In all images, the laser incident laser pulse is traveling right to left with the surface at the left edge of the image. (a) A shockwave at fluences higher ≈20 J/cm^2 was observed at ~500 ns delay from incident laser pulse. (b) Similar behavior at ~500 ns delay was observed for aluminum (b) and tungsten (c) particles with the latter displaying less molten 'spray' as expected from a relatively higher melting point as compared with the former. Fragmentation was also observed for aluminum (d, e), either partial at low fluence or complete at high fluence (e).

Unlike the input surface, particles ablated from the exit surface can be propelled away from the surface under the action of laser initiated and expanding plasma [3]. Generally, the dynamics of laser-microparticle interaction involve high gradients of pressure, temperature and corresponding changes to thermodynamic material properties, plasma formation and aerodynamic effects, necessitating time-resolved measurements. Figure 2 displays shadowgraphy measurements capturing the moment that metal particle contaminants are ablated by the laser pulse and ejected away due to plasma expansion and recoil momentum. Figure 2(a) shows the result for a ~100 J/cm^2, 1064 nm, 7 ns long laser pulse at a delay of ~500 ns where a ~30 μm steel particle ejection as well as the shock front and material spray is visible. Similar behavior was observed for other

metal particles [aluminum: Fig. 2(b); : tungsten Fig. 2(c)]. Along with evidence of material melting and 'spray' shown in Figs. 2(a)-(c), aluminum particles were also observed to fragment as shown in Figs. 2(d) and 2(e).

Because plasma is generated during the ablation/ejection process, it is possible to capture the spectrum of the plasma emission to gain additional information about the ablation/pitting/damage process [6]. Figure 3(a) shows the plasma (electron) temperature derived from a line-to-continuum analysis of the plasma spectrum for Fe atoms in stainless steel 316L [inset of Fig. 3(a)]. As shown, a decrease in plasma temperature vs delay time τ is observed, consistent with an adiabatic expansion of plasma/gas as cooling proceeds after the initial 7 ns laser pulse. More interestingly, by tuning our spectrometer to capture both Fe atomic lines emitted from the particle surface and Si atomic lines emitted from the substrate, we are able to probe temperature inhomogeneities in the plasma as shown in Fig. 3(b). From Fig. 2 it is clear that the plasma generated from the plasma of Fe species is expanding during a time which the particle has not traveled far, implying that the plasma at the silica-steel interface may be confined. Figure 3(b) appears to confirm this assertion since the temperature of the Si species close to the interface is higher than that derived from the Fe which is emitted across a wider area of (unconfined) steel surface.

Similar to the laser-induced shallow sites produced on the input surface discussed earlier, ablation of particles bound to the output surface also created shallow (~10's to 100's of nm deep) pitting and/or optical damage [7, 9]. An remarkable finding of our study of exit surface damage was that, while opaque (e.g. metallic) particles on the input surface ultimately posed the most danger for an optic as compared to semi-transparent particles (e.g. glass), the opposite was true on the exit surface. That is, glass particles ablated on the input surface tended to eject away and not cause catastrophic (i.e. fracture-type, growing) damage, while glass particles on the exit surface tended to explode towards the surface, and create stochastic, micro-fractures which grew upon subsequent shots leading to catastrophic damage [1].
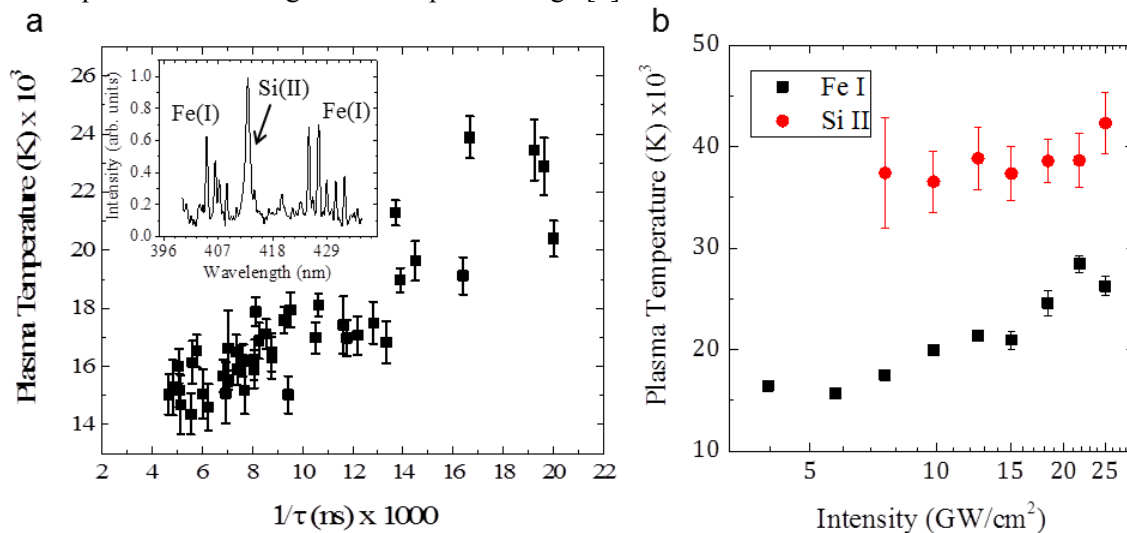

Figure 3: (a) Plasma temperature as a function of inverse gate delay for a 316L steel particle on SiO$_2$ substrate irradiated with single 1064 nm, ~10 GW/cm² laser pulse. The inset shows a typical plasma spectrum used to derive plasma temperature from Fe(I) and Si(II) species. (b) Comparison of temperatures as a function of laser intensity extracted from plasma emission lines related to the substrate (fused silica, Si(II)) and the ejected particle (SS316L, Fe(I))

In contrast, metal particles on the exit surface deterministically led to micro-pits or shallow sites above some threshold (~2 J/cm², 351 nm at 5 ns pulse length). While not leading to catastrophic damage, large ensembles of these micro-pits created after many optic recycles in a large optical

system like NIF can lead to system degradation due to optical loss from scattering [7-9]. A numerical simulation was used to estimate the impact of micro-pit scattering ensembles, and we developed a test bench to measure scattering in test samples to validate our modeling. Figure 4 shows the results of scattering measurements from fused silica samples first contaminated with ~5 μm aluminum spherical particles, then irradiated with 3 pulses of 351 nm, 3 ns long laser light at varying fluence levels. Figure 4(a) shows the raw far-field scattering pattern from our f/20 optical system in which the micro-pitted optic is placed in the near-field; a perfectly non-scattering surface would allow all light passing through the f/20 lens to focus through the central pinhole [shown as the dark central core in Fig. 4(a)]. Figure 4(b) shows scattering lineouts as a function of angle for 2, 5, 8 and 11 J/cm^2 fluence levels, and indicates a larger amount of scattering at higher fluences both due to more particles above pitting threshold and deeper pits formed as a result of the ablation process. In order to compare with our FDTD-based modeling prediction (not shown here but presented in Ref [8]), we characterized the micro-pit ensemble morphologies using laser confocal scanning profilometry, and propagated a 351 nm laser beam through them, finding good agreement between theory and experiment. Interestingly, as indicated by slope A in Fig. 4(b), the highest fluence (~11 J/cm^2) showed a second scattering component to the micro-pit ensemble (slope B), which was found to correlate with the onset of fracture-type damage caused by particle induced Hertzian fractures [2]. Thus, through analysis of the far field scattering angular distribution, pitting/damage types could be deduced without direct imaging of the surface, a fact that might be exploited in damage monitoring schemes for systems engineering purposes in the future [16, 17].
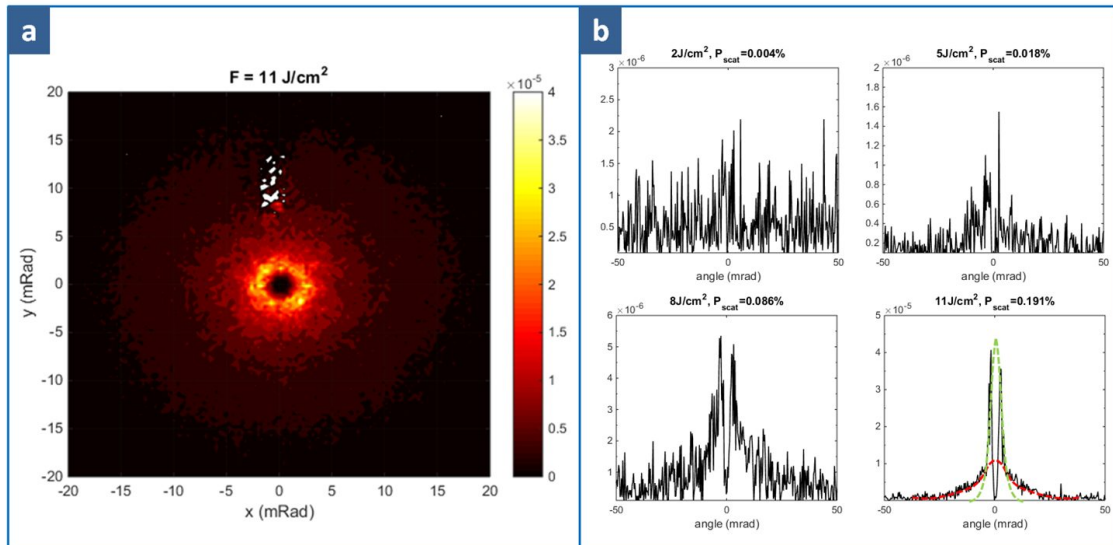

Figure 4: Scatter irradiation from exit surface pitting induced by laser ablation of metal microparticles. (a) the 2D irradiance vs angle of the sample with exposure fluence of 11 J/cm^2. The scattered power is normalized as a fraction of the incident beam power. (b) Profile of the irradiance (through the x-axis) for four samples exposed to 2, 5, 8 and 11 J/cm^2. The scattered power (P_{scat}) as a fraction of the incident beam power is given at the legend in units of % (with the estimated measurement error being 0.015%). The dashed lines illustrate the different contributions of object types to the 11J/cm^2 curve.

Finally, contamination related optical damage and system performance degradation was found to not only be limited to transmission optics, but dielectric high reflective optics as well [4, 5]. Early studies the effect of particulate contamination showed that the laser-induced damage to the reflective surface is strongly dependent on the contaminant type, size and laser fluences [18]; Furthermore, similar to transparent optical components, these contaminant particles when interacting with laser beam, can create pits and damage sites which can lead to beam modulation which can result in further damage on optical components downstream.

The representative metallic contaminants used to study MLDs were spherically-shaped Ti particles which can be generated in high power pulsed laser systems through laser ablation within beam dumps and subsequent deposition of condensed metal vapor on nearby optics. Silica-hafnia multilayer coating samples with different cap layer and high reflectivity (>99.5%) fabricated by e-beam physical vapor deposition were primarily used in our study. Contaminated surfaces were exposed to one ~10 ns, 10 J/cm^2 pulse of laser light (p-polarized, 1053 nm) at an incidence angle of 45°.

Figure 5(a) shows a representative of modified areas on a Ti particle-contaminated MLD surface following a laser pulse containing three adjacent damaged sites with two of which overlapping to each other. At the circumference of each site, the edges are rough and show clear breakage from the host material [Fig. 5(b)]. Higher resolution images of the edges confirm that they are in fact only one layer thick [see Fig. 5(c) for example] which indicates that the interaction between the laser and Ti particle on the coating surface leads to surface modification by delaminating the capping layer. Moreover, within nearly all the damage sites, there remains a pocket or island of Al$_2$O$_3$ capping material that is not damaged [next to the red dots in Fig. 5(a)]. Interestingly, this undamaged pocket is always close to where the Ti particle resides prior to the exposure. This observation suggests that there is a "low energy" spot behind the particle where its existence also provides a protecting shadow for the capping layer that is sitting behind.
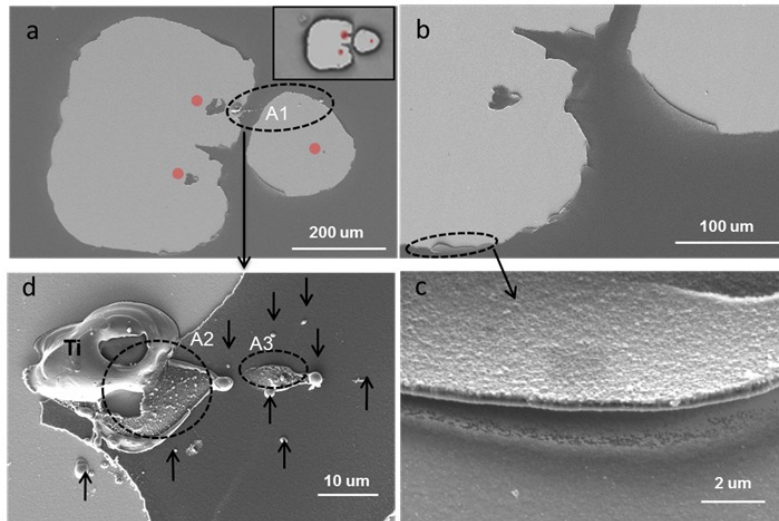

Figure 5: (a) Scanning electron microscopy images displaying the morphology of optical damage on an MLD surface contaminated with Ti particles at different resolutions. The insert is the corresponding optical image. (b) Zoomed in view showing roughened edge of damage site. (c) High resolution image shows the delamination of the top layer. Image was collected at a rotated 180° with respect to others. (d) A close-up view of area A1 shown in (a). Arrows show molten Ti droplets on the surface.

The salient results of the MLD study were that the shape of the particle and the mechanical properties largely dictated the survivability of the MLD film after the first last pulse. Spherical particles were chosen to closely resemble droplets that might form if Ti metal within a beam dump is vaporized from a laser pulse and subsequently condenses. Interestingly, the smooth spherical surface forms a local reflector, sending the 45° light back to the surface and intensifying the local fluence and leading to lower damage thresholds for both overcoat materials studied (Al$_2$O$_3$ and SiO$_2$) [4]. In contrast, irregularly-shaped Ti particles, such as those that might be formed from mechanical abrasion, tended to yield higher damage thresholds. While the higher fracture toughness and strength of Al$_2$O$_3$ relative to SiO$_2$ was expected to provide more resilient surfaces with respect to particle-induced damage, the larger thermal expansion actually led to a higher propensity for damage through delamination.

3. CONCLUSIONS

Particle ablation on exit- and input-surface fused-silica windows in high power laser systems was shown to depend strongly on particle optical properties and orientation. Pump-probe experiment and FDTD simulations of metal and glass particle ejection from fused-silica surfaces was used to understand energy coupling mechanisms which can be used to guide mitigation strategies. Simulated light scattering and intensification associated with particles and pitted surfaces were validated with experiment, and used to develop a quantitative tool for system design purposes. An over-coat design was developed in an attempt to reduce particle-induced damage on multilayer dielectric mirror coatings. Experiments related to MLD mirror coating damage from debris revealed both polarization- and particle morphology-dependent behavior. The results have generated significant interest from industry, in particular related to directed energy and other high power (e.g. LIGO) laser applications.

ACKNOWLEDGEMENTS

REFERENCES

[1]   R. N. Raman, S. G. Demos, N. Shen, E. Feigenbaum, R. A. Negres, S. Elhadj, A. M. Rubenchik, and M. J. Matthews, "Damage on fused silica optics caused by laser ablation of surface-bound microparticles," *Optics Express,* vol. 24, pp. 2634-2647, Feb 8 2016.

[2]   E. Feigenbaum, R. N. Raman, D. Cross, C. W. Carr, and M. J. Matthews, "Laser-induced Hertzian fractures in silica initiated by metal micro-particles on the exit surface," *Optics Express,* vol. 24, May 2016.

[3]   S. G. Demos, R. A. Negres, R. N. Raman, N. Shen, A. M. Rubenchik, and M. J. Matthews, "Mechanisms governing the interaction of metallic particles with nanosecond laser pulses," *Optics Express,* vol. 24, pp. 7792-7815, 2016/04/04 2016.

[4]   S. R. Qiu, M. A. Norton, J. Honig, A. M. Rubenchik, C. D. Boley, A. Rigatti, C. J. Stolz, and M. J. Matthews, "Shape dependence of laser–particle interaction-induced damage on the protective capping layer of 1ω high reflector mirror coatings," *Optical Engineering,* vol. 56, p. 011108, 10/24/2016 2016.

[5]   S. R. Qiu, M. A. Norton, R. N. Raman, A. M. Rubenchik, C. D. Boley, A. Rigatti, P. B. Mirkarimi, C. J. Stolz, and M. J. Matthews, "Impact of laser-contaminant interaction on the performance of the protective capping layer of 1 omega high-reflection mirror coatings," *Applied Optics,* vol. 54, pp. 8607-8616, Oct 2015.

[6]   C. L. Harris, N. Shen, A. Rubenchik, S. G. Demos, and M. J. Matthews, "Characterization of laser-induced plasmas associated with energetic laser cleaning of metal particles on fused silica surfaces," *Optics Letters,* vol. 40, pp. 5212-5215, 2015.

[7]   E. Feigenbaum, R. N. Raman, N. Nielsen, and M. J. Matthews, "Light Scattering from Laser-Induced Shallow Pits on Silica Exit Surfaces," *Laser-Induced Damage in Optical Materials: 2015,* vol. 9632, 2015.

[8]   E. Feigenbaum, N. Nielsen, and M. J. Matthews, "Measurement of optical scattered power from laser-induced shallow pits on silica," *Applied Optics,* vol. 54, pp. 8554-8560, 2015/10/01 2015.

[9]   E. Feigenbaum, S. Elhadj, and M. J. Matthews, "Light scattering from laser induced pit ensembles on high power laser optics," *Optics Express,* vol. 23, pp. 10589-10597, 2015/04/20 2015.

[10]   M. J. Matthews, N. Shen, A. M. Rubenchik, J. Honig, and J. D. Bude, "Phase modulation in high power optical systems caused by pulsed laser-driven particle ablation events," in *SPIE Laser Damage*, 2013, pp. 88850T-88850T-8.

[11]   M. J. Matthews, N. Shen, J. Honig, J. D. Bude, and A. M. Rubenchik, "Phase modulation and morphological evolution associated with surface-bound particle ablation," *JOSA B,* vol. 30, pp. 3233-3242, 2013.

[12]   M. J. Matthews, S. T. Yang, N. Shen, S. Elhadj, R. N. Raman, G. Guss, I. L. Bass, M. C. Nostrand, and P. J. Wegner, "Micro-Shaping, Polishing, and Damage Repair of Fused Silica Surfaces Using Focused Infrared Laser Beams," *Advanced Engineering Materials,* vol. 17, p. 247, 2015.

[13]   M. Matthews, "Simulating laser-material interactions," *Laser Focus World,* vol. 51, pp. 33-38, Aug 2015.

[14]   C. A. Haynam, P. J. Wegner, J. M. Auerbach, M. W. Bowers, S. N. Dixit, G. V. Erbert, G. M. Heestand, M. A. Henesian, M. R. Hermann, K. S. Jancaitis, K. R. Manes, C. D. Marshall, N. C. Mehta, J. Menapace, E. Moses, J. R. Murray, M. C. Nostrand, C. D. Orth, R. Patterson, R. A. Sacks, M. J. Shaw, M. Spaeth, S. B. Sutton, W. H. Williams, C. C. Widmayer, R. K. White, S. T. Yang, and B. M. Van Wonterghem, "National ignition facility laser performance status," *Applied Optics,* vol. 46, pp. 3276-3303, Jun 1 2007.

[15]   S. G. Demos, R. A. Negres, R. N. Raman, M. D. Feit, K. R. Manes, and A. M. Rubenchik, "Morphology of ejected debris from laser super-heated fused silica following exit surface laser-induced damage," 2015, pp. 96320S-96320S-7.

[16]   K. R. Manes, M. L. Spaeth, J. J. Adams, M. W. Bowers, J. D. Bude, C. W. Carr, A. D. Conder, D. A. Cross, S. G. Demos, J. M. G. Di Nicola, S. N. Dixit, E. Feigenbaum, R. G. Finucane, G. M. Guss, M. A. Henesian, J. Honig, D. H. Kalantar, L. M. Kegelmeyer, Z. M. Liao, B. J. MacGowan, M. J. Matthews, K. P. McCandless, N. C. Mehta, P. E. Miller, R. A. Negres, M. A. Norton, M. C. Nostrand, C. D. Orth, R. A. Sacks, M. J. Shaw, L. R. Siegel, C. J. Stolz, T. I. Suratwala, J. B. Trenholme, P. J. Wegner, P. K. Whitman, C. C. Widmayer, and S. T. Yang, "Damage Mechanisms Avoided or Managed for NIF Large Optics," *Fusion Science and Technology,* vol. 69, pp. 146-249, Jan-Feb 2016.

[17]   M. L. Spaeth and T. I. S. P. J. Wegner, M. C. Nostrand, J. D. Bude, A. D. Conder, J. A. Folta, J. E. Heebner, L. M. Kegelmeyer, B. J. MacGowan, D. C. Mason, M. J. Matthews, P. K. Whitman, "Optics Recycle Loop Strategy for NIF Operations Above UV Laser-Induced Damage Threshold," *Fusion Science and Technology,* vol. 69, pp. 265-294, 2016.

[18]   M. A. Norton, C. J. Stolz, E. E. Donohue, W. G. Hollingsworth, K. Listiyo, J. A. Pryatel, and R. P. Hackel, "Impact of contaminates on the laser damage threshold of 1ω HR coatings," 2005, pp. 59910O-59910O-9.